Journal of Thermal Engineering
Web page info: https://jten.yildiz.edu.tr
DOI: 10.18186/thermal.1112660

Research Article

Assessment of microwave susceptors for optimum temperature rise using parametric numerical simulation

Praveen Kumar LOHARKAR[1]*, Asha INGLE[2]

[1]*Department of Mechanical Engineering, SVKM's NMIMS, MPSTME, Shirpur Campus, Dhule, Maharashtra, India*
[2]*Department of Mechanical Engineering, SVKM's NMIMS, MPSTME, Mumbai, Maharashtra, India*

ARTICLE INFO

Article history
Received: 08 October 2021
Accepted: 25 February 2022

Keywords:
Energy Conversion; Microwave; Multiphysics; Susceptors; Regression; Simulation; Volumetric Heating

ABSTRACT

Microwave hybrid heating or indirect microwave heating has been an important development in the processing of metals using microwave energy. In this method of heating, a "susceptor" is used to absorb and convert microwave energy into thermal energy which is utilized for materials processing. Few of these processing applications are sintering, joining, cladding, casting, and composite development. However, the precise selection of a susceptor for a given process is challenging and requires a thorough understanding of the microwave heating phenomenon. In addition, predicting temperature rise in a microwave cavity is a complex task. Numerical simulation can serve to solve these two significant problems. In this work, parametric simulation of microwave heating of three major susceptor materials; silicon carbide, alumina, and coal has been carried out using a multiphysics approach. Initially, a model was developed to validate the simulation procedure. The results were in good agreement with the available data in published literature. Thereafter, the effect of microwave power, position of susceptor block, and time of irradiation on temperature rise in these materials were investigated. On comparing these susceptor blocks after altering the parametric combinations, coal exhibited the formation of hot spots and uneven temperature field with a maximum temperature of 901°C. On the contrary, the temperature attained in silicon carbide (529°C) and alumina (616°C) were lower but distributed in a relatively uniform field across the block. Regression models have also been built to correlate maximum temperature achieved with the parametric variation of parameters. It has been found that microwave power and the time of microwave irradiation have a significant coactive effect on the maximum temperature reached by the material. While the rise in the position of the susceptor block from the base leads to an adverse effect on the temperature rise. The study demonstrates that indirect microwave heating can be harnessed using the proper selection of susceptors as per the temperature requirement of the process. The regression models can be used for the accurate prediction of temperature attainment for given power input, position, and time.

Cite this article as: Loharkar P K, Ingle A. Assessment of microwave susceptors for optimum temperaturerise using parametric numerical simulation. J Ther Eng 2022;8(3):323–334.

***Corresponding author.**
*E-mail address: ploharkar@gmail.com

This paper was recommended for publication in revised form by Regional Editor Baha Zafer

INTRODUCTION

Microwave heating is steadily getting increased attention in the materials processing domain [1,2]. More specifically, in processing applications with metals as primary materials. It offers an effective alternative to processes requiring heat. It can also be used in certain processes involving preheating of materials to avoid thermal stresses during energy-intensive processing, such as laser cladding [3]. In conventional heating applications, the desired rate of heating is achieved either using hot air furnaces; fired by fossil fuels, using electric resistance heating, or induction heating. All these methods consume a large amount of energy, harm the environment, and comprise of large heat losses [4,5].

On the contrary, microwave energy has demonstrated key benefits through its application in several processes involving heat [6,7]. In recent years, several important materials processing applications have been presented utilizing microwave energy. This development is mainly driven by the use of microwave irradiation for metal processing. The advent of metal processing through microwaves is attributed mainly to the realization of two main aspects. One is the use of powdered metals with particle size to the order of depth of microwave penetration [7,8]. While the second one is the practice of indirect microwave heating mechanisms derived from the use of materials known as "susceptors". These materials are microwave absorbers with the ability to convert microwave energy into thermal energy [9].

A few industrial-scale applications utilizing microwave heating have evolved, such as drying and sintering [10]. However, metal processing using microwaves is confined to lab-scale research due to limited technological evolution. The major challenge with microwaves is to control and predict the temperature achieved during the heating process. The subsequent sub-section presents the background of heating accomplished using microwave irradiation.

Microwave Heating-Background

Microwave radiation is a vital and useful constituent of the "electromagnetic" radiation spectrum with characteristically longer wavelengths ranging from 1 mm to 1 m [5]. Its unique abilities make it an inseparable part of many engineering applications including the ones requiring heating. As stated earlier, research on metal-related microwave-based processing applications is very recent and has experienced growth in the past two decades after realizing the concept of hybrid or indirect heating [11,12].

Fundamentally, microwave heating is an outcome of molecular level polarization and conduction [7]. "Polarization" is associated with dipolar movements under the effect of the electric field which is a constituent of radiations that are part of the electromagnetic spectrum; it is also known as "dielectric heating". While "Conduction" is attributed to mobile ions and charges within the influence of the electric field; it is also known as "Ohmic heating" [13]. The efficiency of microwave heating is owing to its ability of "volumetric" heating which is exactly opposite to "conventional" heating wherein heat is directed from the surface to the bulk of the material. Volumetric heating is faster and leads to a uniform temperature field resulting in better properties in processed materials [11]. Figure 1 gives a schematic representation of volumetric heating and conventional heating. In the former case, heat generates at the center and spreads outwards, while in the latter case, heat transfers from outside to the inside of the bulk material.

Sun et al. [7] reported that under the effect of microwave irradiation, materials also experience heating owing to "magnetic" losses and "discharge" related losses as well. The former is caused when the material being processed is magnetic while the latter is caused when the material is electrically conductive.

Thus, dielectric properties and magnetic properties have a profound role in governing temperature rise in irradiated materials. This property is quantified using complex permittivity (ε^*) and complex permeability (μ^*) as depicted in equation 1 and equation 2 respectively.

$$\varepsilon^* = \varepsilon' - j\varepsilon'' \tag{1}$$

$$\mu^* = \mu' - j\mu'' \tag{2}$$

The real term in equation 1; ε' is the dielectric strength which gives the measure of the ability to "store" electric potential energy while the imaginary term, ε'' is the dielectric loss which gives the measure of the ability to "convert" the stored energy into the thermal form [5]. In equation 2, the real term (μ') corresponds to the storage of energy while the imaginary term (μ'') signifies the amount of loss of energy that results in heating.

There is another important property derived from complex permittivity and complex permeability called "losstangent". It is the ratio of the imaginary term and the real term of the two equations. If the value of loss tangents is

(a) **(b)**

Figure 1. (a)Volumetric heating versus (b) conventional heating.

small, the corresponding materials are not suitable for direct microwave heating. To process such materials, an indirect heating technique or a hybrid heating technique using "susceptors" is employed whereby the desired transformation of electromagnetic energy to heat is achieved. This heat is then transferred to the low-loss material by conventional heat transfer modes [14].

There are several alternatives for "susceptors" discussed in the literature with varying interaction capabilitiesunder microwave environments [9,15,16]. This leads to a different amount of temperature rise. The use of numerical simulation in electromagnetics has been demonstrated especially in the field of communication and to some extent infood processing research [17,18]. In recent years, researchers have used this multiphysics simulation approach for the prediction of temperature rise in materials such as, "Coal" [19], "Asphalt" [20], "Biomass" [21], etc. In all these studies, the focus had been to study temperature rise in the chosen materials subjected to direct exposure to microwaveradiation. For instance, in the study done by Hong et al. [19], 3-D simulation of coal heating was carried out to understand the effect of parameters. In this study it was demonstrated that position is key to achieve efficient heating of specimen. Similarly, simulation study on microwave heating of biomass was presented by Halim and Swithenbank[21]. In this work, temperature field for biomass was evaluated for different dielectric properties of the material and position inside the cavity. The study was proposed to be one of the initial parametric studies on microwave heating ofbiomass. However, with reference to all these studies, not much literature is available on development of regression models and to assess the relative temperature rise in the susceptors used for metal processing and their relative comparison.

A numerical simulation-based study to evaluate the prominent susceptors can be significant to establish the microwave heating process at an industrial scale. It is also imperative to devise a reliable model to predict the temperature achieved during such processes. In addition, the effect of varying process parameters such as microwave power, the position of susceptor block inside the microwave cavity, and irradiation time would consolidate understanding of the microwave heating process.

Furthermore, it is recognized that numerical simulation of susceptor heating can help in speeding up the research on microwave-based metal processing. Therefore, in this work, parametric numerical simulation of susceptor heating derived from microwaves is carried out under different parametric conditions. The objective has been to compare various prominent susceptors for potential large-scale applications and study the effect of input power, irradiation time, and block position inside the cavity on the temperature rise. A mathematical model to relate the maximum temperature reached during the microwave heating process as a function of the chosen parameters is also developed for the three susceptor materials.

MODELING OF MICROWAVE HEATING OF SUSCEPTORS

The steps necessary for numerical simulation of heating from microwaves, are shown in Figure 2 [22]. Microwave heating involves two important physical phenomena; one related to the movement of electromagnetic waves and the other related to heat transfer. It is imperative to couple these two physics be able to simulate the microwave heating process and hence a multiphysics processing approach is required. Detailed discussion on these steps is presented in the following sub-sections.

Model Generation

The first step in the analysis was to develop a multiphysics model of the microwave oven cavity with a susceptor. Three susceptors that have been extensively used in several microwave processing applications, viz. silicon carbide, alumina, and coal [9] were modeled.

The susceptors have been modeled as a block of size 100×50×50 cubic mm for assessment of temperature rise. Figure 3 depicts the model of the microwave oven with the susceptor. The rectangular cross-section port at the top right-hand side receives the electromagnetic power input at a frequency of 2450 MHz, which is the designated frequency for microwave heating applications [23]. The port operates at TE10 mode. Here TE translates to transverse electric, that is, electric field traverses in a direction transverse to the direction of wave propagation. This mode of wave propagation is dominant for the frequency of 2450

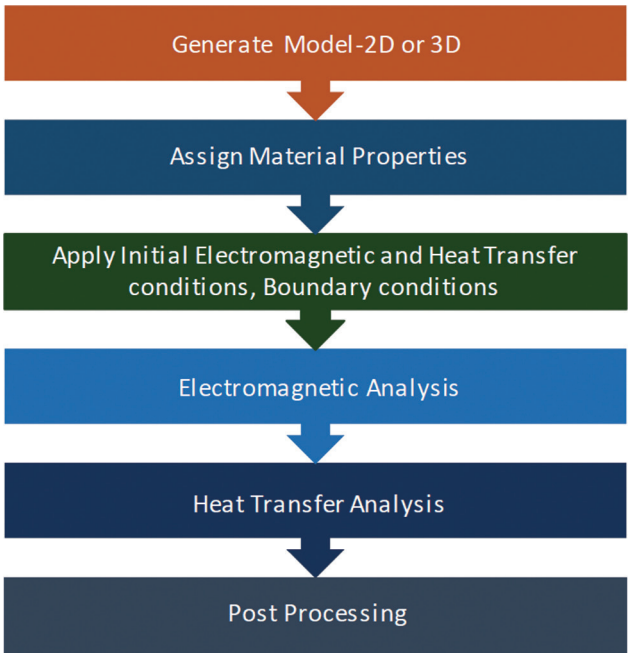

Figure 2. Steps in microwave heating simulation (modified from [22]).

MHz and rectangular geometry of the port [24]. Following assumptions have been made during the modeling of the susceptor heating system.

- The susceptor materials are homogeneous and isotropic.
- The heat transfer is limited to the susceptor material.
- The material properties such as dielectric constant, heat capacity at constant pressure, thermal conductivity remain constant for the duration of irradiation.
- The susceptor material is linearly elastic.

Material Properties

Assigning material properties is critical to analysis and a key step in pre-processing for any finite element- based numerical simulation. The properties of three susceptors; silicon carbide, coal, and alumina were obtained from the data available in the available literature [25,26]. *Table 1* shows the properties of these materials. As stated in the assumptions, the material properties were assumed to be time-independent.

The other components of the model, such as the microwave cavity and walls of the microwave oven were modeled using properties of air and copper respectively which are in-built in the software package. The properties of the glass plate were taken from the application library of the package.

Model Governing Equations

Microwave heating simulation requires finding a solution to a multiphysics problem having equations that govern electromagnetic wave propagation and the equations that govern heat transfer in the materials. Electromagnetic wave propagation is described by Maxwell's equations. Equation 3 governs the distribution of electric fields within the microwave oven cavity [27].

$$\nabla \times \mu_r^{-1}(\nabla \times E) - k_0^2\left(\varepsilon_r - \frac{j\sigma}{\varepsilon_0}\right)E = 0 \tag{3}$$

Here, μ_r is relative permeability, E is the intensity of electric field in Vm^{-1}, ε_r is the relative permittivity; σ depicts the electrical conductivity in Sm^{-1}, ω is the radiation's angular frequency in $rads^{-1}$ and ε_0 is the free space permittivity (8.85×10^{-12} Fm^{-1}). k_0 represents wave number in a vacuum and is given as (refer to equation 4):

$$k_0 = \frac{\omega}{c_0} \tag{4}$$

where c_0 represents the speed of light (2.998×10^8 ms^{-1}) in a vacuum.

Now, to evaluate temperature rise in the susceptor block, the heat transfer equation based on Fourier's law of heat conduction is to be evaluated [22]. The corresponding equation used for heat transfer in solids is expressed as follows (equation 5).

$$\rho C_p \frac{\partial T}{\partial t} + \rho C_p u.\nabla T + \nabla.q = Q_{ted} \tag{5}$$

Where ρ is the density of susceptor block in kgm^{-3}, C_p is the specific heat capacity at constant pressure in $Jkg^{-1}K^{-1}$, T is the absolute temperature in K, Q_{ted} represents heat from microwave energy in Wm^{-3}, and q is heat flux in Wm^{-2}; it is depicted by equation 6.

$$q = -k\nabla T \tag{6}$$

Where k is thermal conductivity in $Wm^{-1}K^{-1}$

Boundary and Initial Conditions

The problem involving heating of materials inside a microwave cavity exhibits symmetricity which allows for

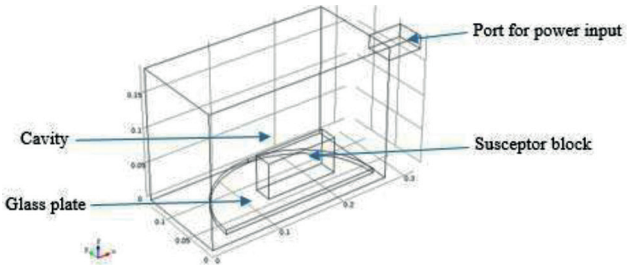

Figure 3. Model of the microwave oven with the susceptor.

Table 1. Properties of susceptors

Property	Silicon Carbide [25]	Alumina [25]	Coal [26]
Relative permittivity; ε_r	9.6	8.9	2.86–0.17j
Relative permeability; μ_r	1	1	1
Electrical conductivity; σ(Sm^{-1})	0.02	0.27	10–3
Thermal conductivity; k ($Wm^{-1}K^{-1}$)	250	27	0.189
Material density; ρ (kgm^{-3})	3210	3900	1310
Specific heat capacity; C_p ($Jkg^{-1}K^{-1}$)	1000	900	4187

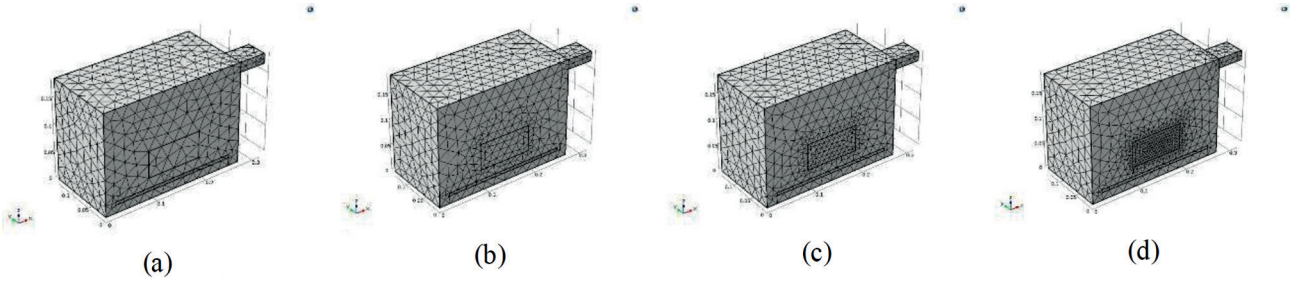

Figure 4. Grid-independence study: (a) coarser mesh, (b) finer mesh, (c) extra fine mesh and (d) extremely fine mesh.

modeling only one-half of the heating setup. A boundary condition shown by equation 7 was used to include this effect.

$$n \times H = 0 \tag{7}$$

Where, H is magnetic field intensity in Am^{-1}.

The walls of the oven and the port were assigned impedance boundary conditions that confine the microwaves within the cavity. This condition is represented by equation 8.

$$\frac{\mu_0 \mu_r}{\sqrt{\varepsilon_0 \varepsilon_r} - \frac{j\sigma}{\omega}} n \times H + E - (n.E)n = 0 \tag{8}$$

Where the symbols have their usual meaning as described after equations 2 and 7. Initial electric field intensity was taken as 0.

Referring to Figure 3, microwave radiations enter inside the cavity through the port. The wave is controlled using a propagation constant given by the equation 9, which is:

$$\beta = \frac{2\pi}{C_0} \sqrt{v^2 - v_c^2} \tag{9}$$

where β is the propagation constant; v is the frequency of microwave in cps; v_c. is the cut-off frequency in cps.

For the heat transfer in susceptor block, thermal insulation boundary condition was introduced which denotes that no heat flux exists across the boundary. The condition is represented using the following equation 10.

$$-n.\left(-k \nabla T\right) = 0 \tag{10}$$

Effectively, this equation signifies that there is no temperature gradient across the boundary. In other words, the temperature on either side of the boundaries must be equal. The initial temperature of the susceptor block was kept to be 25°C.

Meshing and Grid Independence Study

A tetrahedral mesh was used to discretize the model. To ensure that mesh size or the number of elements doesn't cause significant error in temperature prediction, a grid-independent study was carried out on all the three susceptor blocks with varying mesh size/number of elements. Figure 4a, Figure 4b, Figure 4c, and Figure 4d represent the models with coarser mesh, finer mesh, extra fine mesh, and extremely fine mesh respectively.

Figures 5a, 5b, 5c, and 5d depict the temperature attained for the various mesh sizes for silicon carbide block radiated with microwaves at power input (P_{input}) of 700 W for 300 s and positioned just over the glass plate (h = 15 mm). It can be seen that the maximum temperature attained during the simulation varied from 470°C (Coarser), 518°C (Finer), 527°C (Extra fine) to 529°C (Extremely fine). Thus illustrating that the change in maximum temperature got fairly negligible with values being close to each other with the mesh getting finer which relates to the mesh independence of the model [28].

A similar simulation was carried out for the other two susceptor blocks. *Table 2* presents the summary of the grid independence study for all the three materials. It is evident that at extremely fine mesh size, the temperature values got steadied. Hence, for carrying out the parametric sweep, susceptor blocks were meshed with extremely fine elements.

DESIGN OF SIMULATION

Trials were performed based on the concept of "design of experiments" and a regression model was developed to relate temperature with the three input parameters. *Table 3* presents the three parameters or factors (as termed in design of experiments) and their levels used to develop parametric simulation conditions. The power input values, denoted by "P_{input}" were taken as 350 W, 490 W, and 700 W which correspond to 50%, 70%, and 100% settings of the microwave oven with a 700 W rating. The positions of the sample from the base, symbolized by "h" were chosen such that these were equally spaced within the vertical space of the microwave cavity to map the effect of positional

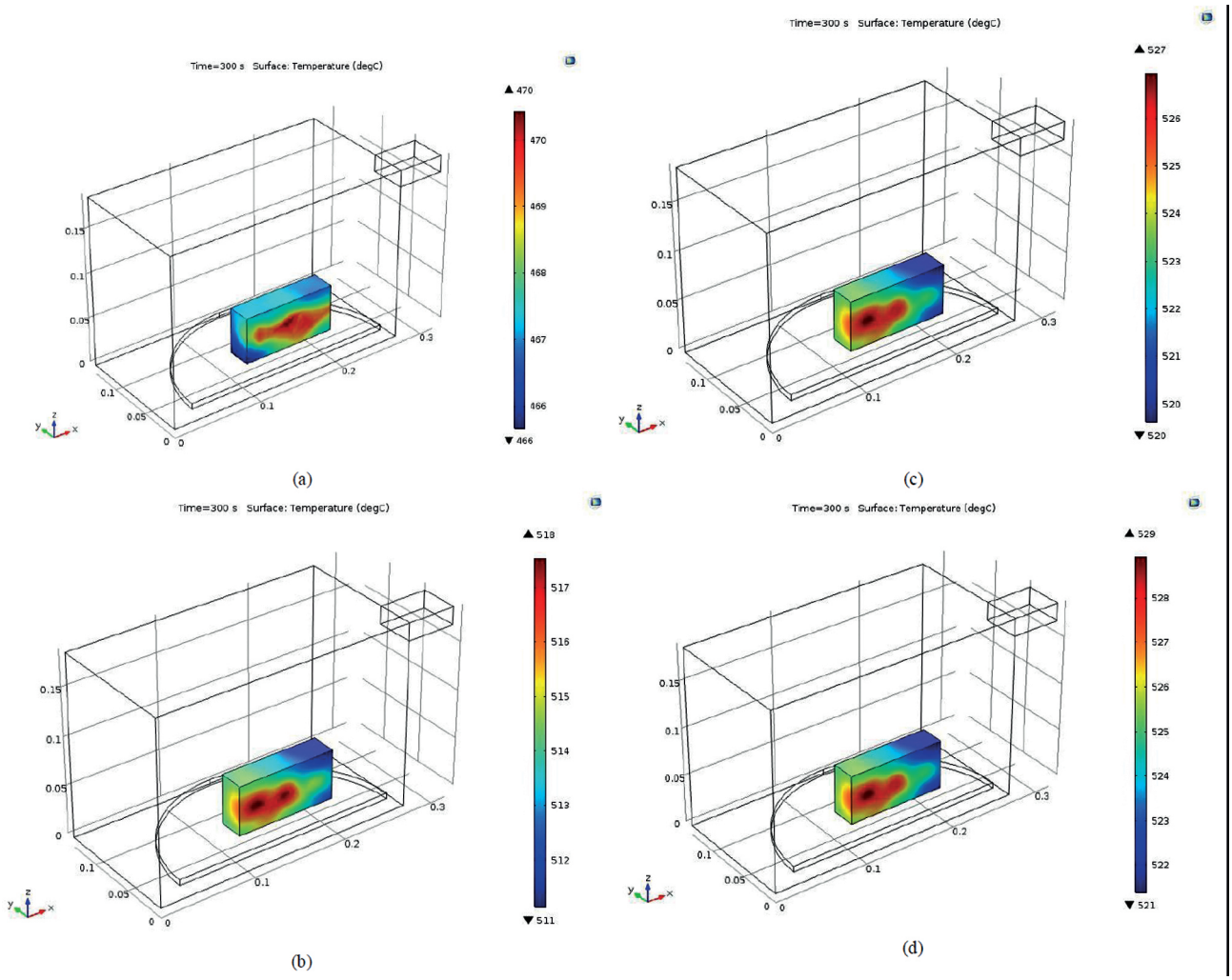

Figure 5. Temperature rise in silicon carbide susceptor for (a) coarser mesh, (b) finer mesh, (c) extra fine mesh and (d) extremely fine mesh at t = 300, h = 15 mm and P_{input} = 700 W.

Table 2. Summary of grid independence study

Mesh quality	No. of elements	Silicon Carbide	Alumina	Coal
		Maximum temperature attained (in °C)		
Coarser	10377	470	613	922
Finer	11629	518	614	901
Extra Fine	14485	527	615	902
Extremely Fine	25545	529	616	901

Table 3. Parameters and their levels

Parameters	Levels					
P_{input} (W)	350		490		700	
Position of the block from the base, h (mm)	15		60		105	
Irradiation time, t (s)	50	100	150	200	250	300

variation. Positional variation was chosen as a parameter based on the understanding that microwave intensity varies with the position of the load as emphasized in the published literature [2,6,19]. The third parameter was taken as 'irradiation time', 't' to evaluate temperature variation with time.

Microwave heating simulation comprises two study steps. The first one is a frequency-domain study step which takes care of the electromagnetic part of the analysis. While the second study step is a time-dependent one. The latter step is used to analyze the heat-transfer during the simulation. Parametric sweep capability of the software package was used to investigate the consequence

of variation of the chosen parameters on the electric field intensity and the temperature rise in the susceptor blocks.

Model validation was carried out by comparing the simulation results with the published results on microwave heating of a coal specimen with cylindrical geometry. Figure 6 shows the temperature field for the specimen with a height of 60 mm and radius of 25 mm as described by Huang et al. [26]. The power input for the study was taken as 500 W and the time of irradiation was taken as 300 seconds. The frequency of radiation was kept at 2450 MHz. It is evident from Figure 6 that the maximum temperature obtained in the coal specimen is around 611°C which was found to be in close agreement with the published result of 608.908°C. Apart from the maximum temperature, the distribution of temperature (maximum to minimum value) and the location of the hot spot is the same as that published in the study presented by Huang et al. [26]. Thus the procedure was employed to assess temperature distribution in three susceptor materials. The obtained results were used to develop regression models describing the maximum temperature attained based on parametric analysis for each of the susceptor materials. The subsequent section presents the results and related discussion.

RESULTS AND DISCUSSION

The coupled multiphysics models were simulated by applying "parametric sweep" using the parameters stated in *Table 3*. In this study, two field distributions were obtained for evaluation of the parametric effect on microwave heating of susceptors. First one is the electric field distribution and the other one is temperature field distribution across the susceptors.

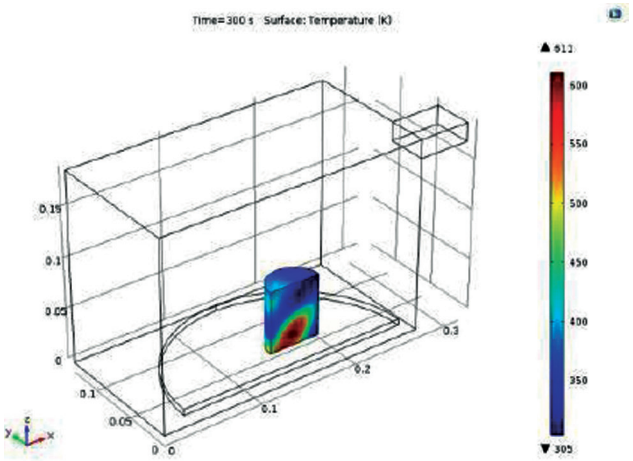

Figure 6. Temperature distribution in a cylindrical specimen modeled for validation.

Since microwave is an electromagnetic radiation, electric field distribution has a profound impact on the temperature field. As discussed in the introduction section, microwave heating is a function of a material's dielectric

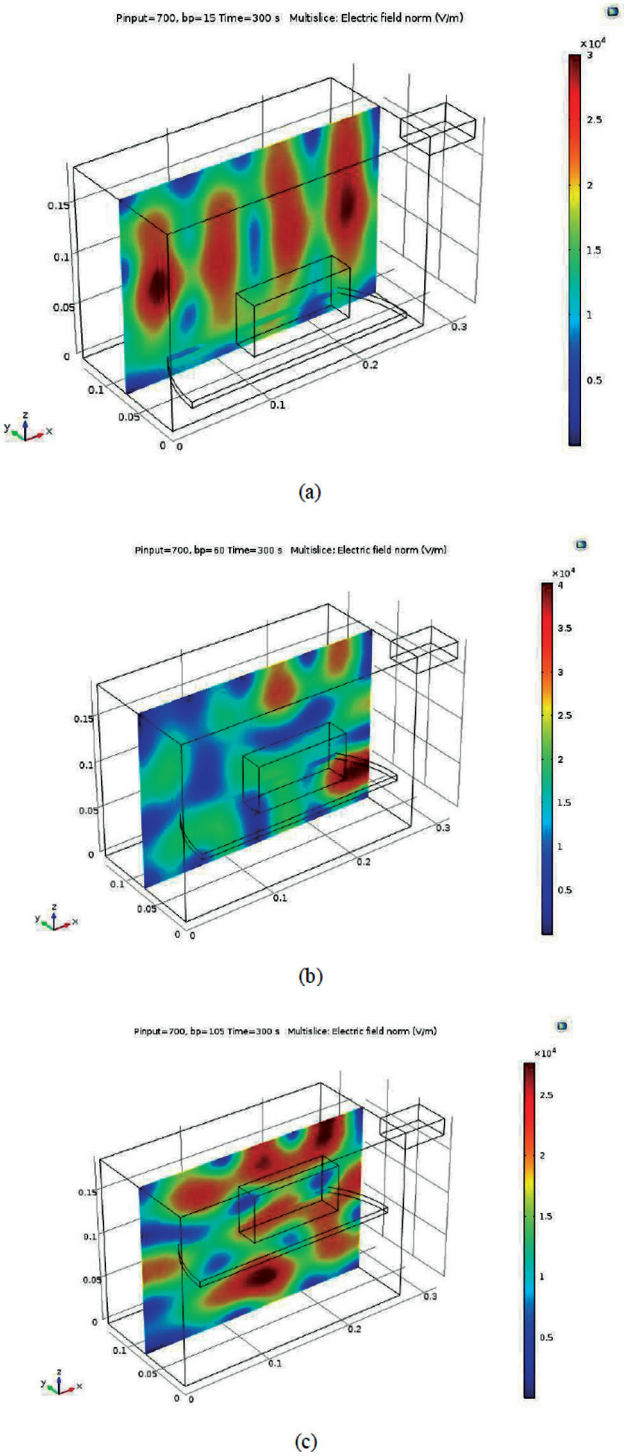

(a)

(b)

(c)

Figure 7. Distribution of electric field (V/m) for silicon carbide at (a) h = 15 mm (b) h = 60 mm (c) h = 105 mm for P_{input} = 700 W and t = 300 s.

properties. Hence, the interaction of materials with the electric field intensity leads to the conversion of microwave energy into thermal energy. That is, higher intensity of the electric field at a given spatial location would result in greater dielectric losses and higher temperatures. Thus distribution of electric field gives an important indication for optimum positioning of the specimen.

In Figure 7a, Figure 7b, and Figure 7c, the electric field distribution for the silicon carbide susceptor positioned at 15 mm, 60 mm, 105 mm respectively from the base and 700 W-microwave power and 300 s- irradiation time.

From Figure 7a, the maximum intensity of electric field around the susceptor block is seen to be in the range ($2 \times 10^4 - 2.5 \times 10^4$) Vm^{-1} for 'h' equal to 15 mm which reduces to ($1 \times 10^4 - 2 \times 10^4$) Vm^{-1} for 'h' equal to 60 mm (refer to Figure 7b) and increases slightly to ($1.5 \times 10^4 - 2.5 \times 10^4$) Vm^{-1} for 'h' equal to 105 mm (refer to Figure 7c).

If we plot the graph (refer to Figure 8) for maximum temperature attained corresponding to the three positions of silicon carbide susceptor block, the position, 'h'= 15

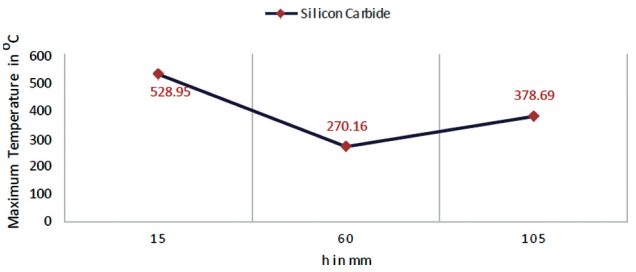

Figure 8. Maximum temperature in silicon carbide versus position of susceptor block at P_{input} = 700 W and t = 300 s.

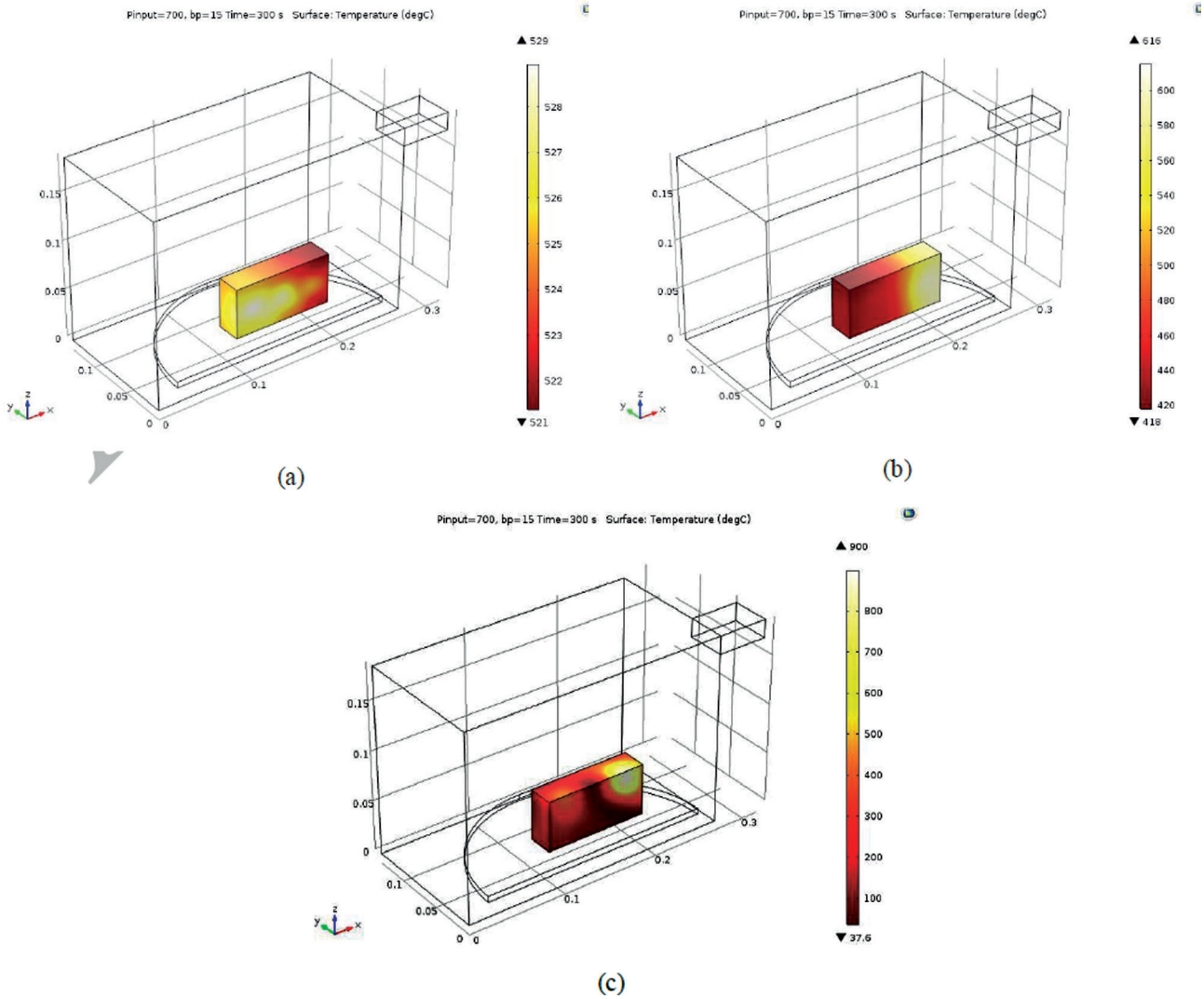

Figure 9. Distribution of temperature field (°C) in (a) silicon carbide (b)alumina and (c) coal for h=15 mm, P_{input} = 700 W and t = 300 s.

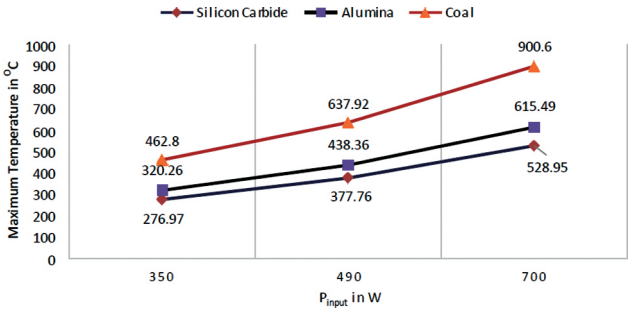

Figure 10. Maximum Temperature v/s Power input for different susceptor materials at h = 15 mm.

mm results in the highest temperature for the given power input and time (700 W, 300 s) which is attributed to greater dielectric loss owing to higher intensity of electric field as shown in Figure 7a. On the contrary, there is a drop in temperature for the position, 'h'= 60 mm owing to the lowered intensity of the electric field at the given location. There is a slight increase in the temperature for 'h' =100 mm which can be attributed to more losses owing to an increase in average intensity of electric field across the block leading to the enhanced transformation of electromagnetic energy to thermal energy.

The effect of material properties of susceptors can be understood and visualized with the help of Figure 9 a, Figure 9 b, and Figure 9c. Herein, the input power and position of the block were kept fixed at 700 W and 300 s respectively. Coal exhibits a larger magnitude of maximum temperature for the given parametric conditions which is further highlighted in Figure 10. This is clearly due to the imaginary term of permittivity which causes loss in electromagnetic energy. Furthermore, the variation in temperature across the block is quite extreme for coal which signifies the existence of severe hot and cold spots across the coal block. On the other hand, silicon carbide and alumina show relatively uniform variations in temperature distribution across the corresponding blocks. This can be due to uneven electric field intensity which leads to localized heating. However, due to higher conductivities, temperature uniformity is better for alumina and silicon carbide as against coal which has very low thermal conductivity.

In Figure 10, variations of maximum temperature against different levels of power input have been plotted. It further emphasizes the effect of the dielectric loss factor. X-axis depicts the three levels of power input and the Y- axis shows the maximum temperature attained in each of the susceptor blocks. It is revealed that at all the power levels, coal exhibits a higher maximum temperature which goes on the decrease for alumina and silicon carbide. This reduction can be explained based on the dielectric and thermal properties of the three materials. Due to the higher

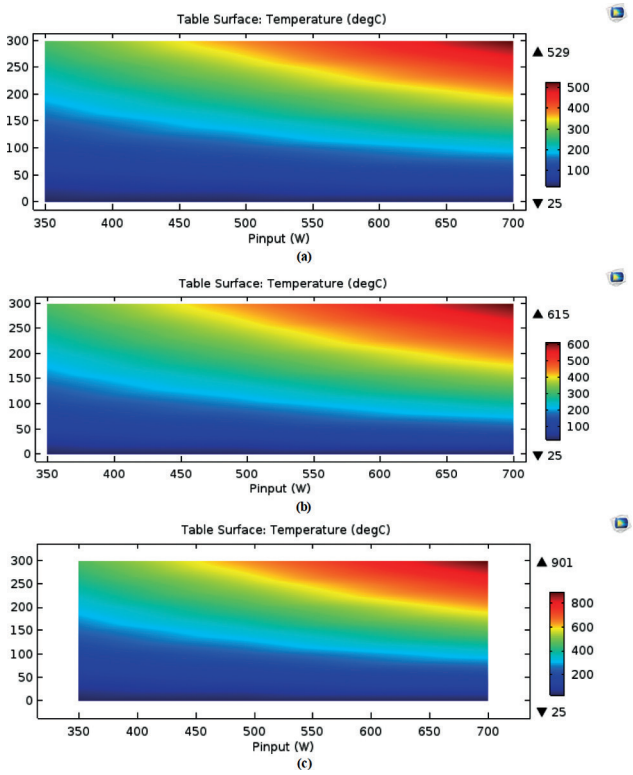

Figure 11. Temperature rise in (a) silicon carbide, (b) alumina, and (c) coal versus P_{input} (W) and t (s) for h = 15 mm.

value of dielectric loss in coal, there is a greater transformation of electromagnetic energy to heat in coal as compared to the other two susceptors.

It can also be understood by these results that pure alumina can lead to relatively high temperatures upon interaction with microwave radiation. Therefore, alumina bricks used as an insulation material tend to have only 30- 40% alumina to avoid damage to the cavity due to excessive heating.

The maximum temperature values obtained from the simulation were recorded. To understand the significance of individual parameters, regression analysis was carried out for the tabulated data using Minitab software. Following equations were obtained for the maximum temperature rise in each susceptor block material; Equation 11 for silicon carbide, equation 12 for alumina, and equation 13 for coal.

$$T_{max} \text{ for Silicon Carbide(°C,)} = -72.7 + 0.8952\ t(s) + 0.2646\ P_{input}\ (W) - 0.610\ h\ (mm) \quad (11)$$

R_{square} was obtained as 79.99%.

$$T_{max} \text{ for Alumina (°C,)} = -145.5 + 1.2831\ t(s) + 0.4082\ P_{input}\ (W) - 0.368\ h\ (mm) \quad (12)$$

R_{square} was obtained as 92.51%.

T_{max} for Coal (°C,) = –36.3 + 1.434 t(s)+ 0.4265
P_{input} (W) –2.564 h (mm) (13)
R_{square} was obtained as 83.40%.

Where 'T_{max}' (°C) is the maximum temperature, 'P_{input}' (W) is the input microwave power, 'h'(mm) is the position of the block from the base of the oven, 't' (s) is the time of irradiation.

For all these regression models, 'p' values were obtained for the coefficients of parameters. These were found to be less than 0.05 for all the coefficients. It implies that all the three chosen parameters have a significant effect on the maximum temperature attained by the three susceptor blocks. The sign of the coefficients revealed that input microwave power and irradiation time of the microwaves has a coactive effect on the temperature rise. This is true to the physics as the microwave energy available for conversion into thermal energy increases with the input microwave power and the time of irradiation. Conversely, the block position has an antagonistic effect which was discussed earlier to be due to the reduced intensity of electric field. Moreover, R_{square} values for all the three regression models were almost equal to or greater than 80% which stresses the fact that the parameters used have a significant impact on the response variable, that is, T_{max}.

For graphical visualization of parametric effects, contour diagrams were plotted (refer to Figure 11a, Figure 11b, and Figure 11c). These plots show the variation of temperature in silicon carbide, alumina, and coal blocks as a function of input power and time. All three figures clearly emphasize the influence of input power and irradiation on the maximum temperature attained in these blocks.

CONCLUSION

Selecting an appropriate susceptor for any microwave processing application is a challenging task. An electromagnetic analysis coupled with heat transfer has been used to compare three prominent susceptors, viz. silicon carbide, alumina, and coal to find out the maximum temperature rise. Regression analysis for the temperature rise in the susceptor blocks has also been carried out to derive temperature as a function of chosen parameters.

It has been inferred that microwave power and time of microwave irradiation are the two most influencing factors in microwave heating while the position of the susceptor block also has a significant effect on the maximum temperature values.

In the context of block position, the lowest position was found to be most effective ('h'= 15 mm) for attaining high temperature while power input of 700 W and time of 300 seconds led to maximum temperatures in the susceptor blocks. Coal exhibited the highest temperature at 901°C followed by alumina at 615°C and silicon carbide at 529°C. However, it is important to note that poor thermal conductivity in coal causes the generation of hot spots and non-uniform temperature fields which is undesirable and not suitable for hybrid microwave heating.

The variation in temperature at different parametric combinations in different materials can be explained in terms of variation in the electric field intensities at those points. Reduced electric field intensities result in lower losses and thus reduce the conversion of microwave energy to thermal energy.

The regression equations developed for all the three susceptor blacks have statistically significant coefficients for the parameters and thus can be used to predict and control the temperature rise. This would help to attain heating at the desired rate while using a particular susceptor. These models can be used as a reference for designing set-ups for various hybrid heating applications and can help to address the issue of reliability of microwave heating in materials processing applications.

NOMENCLATURE

E	Electric field intensity, Vm^{-1}
C_p	Specific heat capacity, $Jkg^{-1}K^{-1}$
q	Rate of heat flux, Wm^{-2}
k	Thermal conductivity, $Wm^{-1}K^{-1}$
t	Irradiation time, s
T	Temperature, °C
T_{max}	Maximum temperature in the susceptor block, °C
P_{input}	Microwave power, W
h	Position of the block from the base, mm
Q_{ted}	Thermoelastic damping, Wm^{-3}
u	Fluid velocity vector, ms^{-1}
μ_r	Relative magnetic permeability, dimensionless

Greek Symbols

ε^*	Complex permittivity, dimensionless
ε'	Dielectric constant of the material, dimensionless
ε_0	Free space permittivity, 8.852 × 10–12, Fm^{-1}
ε''	Dielectric loss factor, dimensionless
ω	Angular frequency of radiations, $rads^{-1}$
σ	Electrical conductivity, Sm^{-1}
ρ	Material density, kgm^{-3}

ACKNOWLEDGMENT

The manuscript is a part of research work funded by SVKM's NMIMS (Deemed-to-be University), Mumbai, India. The authors would like to thank the university for providing the support. The authors are also thankful to Mr. Himanshu Singh, Research Scholar, VNIT Nagpur, India for providing help related to simulation.

AUTHORSHIP CONTRIBUTIONS

Authors equally contributed to this work.

DATA AVAILABILITY STATEMENT

The authors confirm that the data that supports the findings of this study are available within the article. Raw data that support the finding of this study are available from the corresponding author, upon reasonable request.

CONFLICT OF INTEREST

The author declared no potential conflicts of interest with respect to the research, authorship, and/or publication of this article.

ETHICS

There are no ethical issues with the publication of this manuscript.

REFERENCES

[1] El Khaled D, Novas N, Gazquez JA, Manzano-Agugliaro F. Microwave dielectric heating: Applications on metals processing. Renew Sustain Energy Rev 2018;82:2880–2892. [CrossRef]

[2] Loharkar PK, Ingle A, Jhavar S. Parametric review of microwave-based materials processing and its applications. J Mater Res Technol 2019;8:3306–3326. [CrossRef]

[3] Ding C, Cui X, Jiao J, Zhu P. Effects of substrate preheating temperatures on the microstructure, properties, and residual stress of 12CrNi2 prepared by laser cladding deposition technique. Materials (Basel) 2018;11:2401. [CrossRef]

[4] Loharkar PK, Ingle A. Microwave-assisted corrosion resistant pure polyester coating of cold rolled closed annealed steel. Mater Today Proc 2021;44:1676–1680. [CrossRef]

[5] Chandrasekaran S, Ramanathan S, Basak T. Microwave material processing-a review. AIChE J 2012;58:330–363. [CrossRef]

[6] Chandrasekaran S, Basak T, Ramanathan S. Experimental and theoretical investigation on microwave melting of metals. J Mater Process Technol 2011;211:482–487. [CrossRef]

[7] Sun J, Wang W, Yue Q. Review on microwave-matter interaction fundamentals and efficient microwave-associated heating strategies. Materials (Basel) 2016;9:231. [CrossRef]

[8] Singh S, Gupta D, Jain V. Recent applications of microwaves in materials joining and surface coatings. Proc Inst Mech Eng Part B J Eng Manuf 2016;230:603–617. [CrossRef]

[9] Yahaya B, Izman S, Konneh M, Redzuan N. Microwave Hybrid Heating of Materials Using Susceptors - A Brief Review. Adv Mater Res 2013;845:426–430. [CrossRef]

[10] Singh S, Gupta D, Jain V, Sharma AK. Microwave processing of materials and applications in manufacturing industries: A Review. Mater Manuf Process 2015;30:1–29. [CrossRef]

[11] Thostenson ET, Chou T-W. Microwave processing: fundamentals and applications. Compos Part A Appl Sci Manuf 1999;30:1055–1071. [CrossRef]

[12] Roy R, Agrawal D, Cheng J, Gedevanlshvili S. Full sintering of powdered-metal bodies in a microwave field. Nature 1999;399:668–670. [CrossRef]

[13] Reeja-Jayan B, Harrison KL, Yang K, Wang CL, Yilmaz AE, Manthiram A. Microwave-assisted low-temperature growth of thin films in solution. Sci Rep 2012;2:1003. [CrossRef]

[14] Gupta D, Sharma AK. Development and microstructural characterization of microwave cladding on austenitic stainless steel. Surf Coatings Technol 2011;205:5147–5155. [CrossRef]

[15] Dębowski MA. Low temperature microwave processing of silicone resin coatings containing microwave susceptors. Surf Coatings Technol 2017;320:13–17. [CrossRef]

[16] Chandrasekaran S, Basak T, Srinivasan R. Microwave heating characteristics of graphite based powder mixtures. Int Commun Heat Mass Transf 2013;48:22–27. [CrossRef]

[17] Liu S, Fukuoka M, Sakai N. A finite element model for simulating temperature distributions in rotating food during microwave heating. J Food Eng 2013;115:49–62. [CrossRef]

[18] Pitchai K. Electromagnetic and heat transfer modeling of microwave heating in domestic ovens. Dissertations, These. Student Research in Food Science and Technology, 2011.

[19] Hong YD, Lin BQ, Li H, Dai HM, Zhu CJ, Yao H. Three-dimensional simulation of microwave heating coal sample with varying parameters. Appl Therm Eng 2016;93:1145–1154. [CrossRef]

[20] Wang H, Zhang Y, Zhang Y, Feng S, Lu G, Cao L. Laboratory and numerical investigation of microwave heating properties of asphalt mixture. Materials 2019;12:146. [CrossRef]

[21] Halim SA, Swithenbank J. Simulation study of parameters influencing microwave heating of biomass. J Energy Inst 2018:1–22.

[22] Loharkar PK, Ingle A. Numerical analysis of microwave heating: Fundamentals and applications. IOP Conf Ser Mater Sci Eng 2020;810:012061. [CrossRef]

[23] National Research Council. Microwave Processing of Materials. Washington, DC: The National Academies Press, 1994.

[24] Surducan V, Surducan E, Ciupa R, Neamtu C. Microwave generator for scientific and medical applications. AIP Conf Proc 2012;1425:89–92. [CrossRef]

[25] Mishra RR, Sharma AK. On melting characteristics of bulk Al-7039 alloy during in-situ microwave casting. Appl Therm Eng 2017;111:660–675. [CrossRef]

[26] Jinxin H, Guang X, Yinping C, Zhongwei C. International Journal of Mining Science and Technology Simulation of microwave's heating effect on coal seam permeability enhancement. Int J Min Sci Technol 2019;29:785–789. [CrossRef]

[27] Huang J, Xu G, Hu G, Kizil M, Chen Z. A coupled electromagnetic irradiation, heat and mass transfer model for microwave heating and its numerical simulation on coal. Fuel Process Technol 2018;177:237–245.

[28] Regue HM, Bouali B, Benchatti T, Benchatti A. Analysis and simulation of thermal performance of a PTC with secondary reflector. J Therm Eng 2021;7:1531–1540. [CrossRef]